# Flexural response of double-wythe insulated ultra-high-performance concrete panels with low to moderate composite action

Valon Sylaj, Amir Fam, Malcolm Hachborn, and Robert Burak

- This paper proposes a new double-wythe precast concrete panel design using ultra-high-performance concrete and thin wythes to reduce panel weight.
- Eight specimens with varying design parameters, including fiber type, insulation thickness, flexural reinforcement ratio, and shear connector type, were tested in bending to evaluate structural performance.
- The results of the flexural performance testing indicated that including flexural reinforcement in the wythes, increasing insulation thickness, or providing diagonal load paths with the shear connectors can significantly increase the ultimate capacity of the panels.

*PCI Journal* (ISSN 0887-9672) V. 65, No. 1, January–February 2020.
*PCI Journal* is published bimonthly by the Precast/Prestressed Concrete Institute, 200 W. Adams St., Suite 2100, Chicago, IL 60606.


A typical precast concrete insulated wall consists of the exterior concrete layer, referred to as the architectural or facade wythe; the interior concrete wythe, which could be load bearing; and a rigid insulation sandwiched between the wythes. Precast concrete panels are usually used as exterior walls, spanning from the foundation to the floor or from column to column in a structure.[1–3] The overall thickness of the panel is determined based on the applied loads, the thermal performance requirements, and the expected level of composite action between concrete layers. The type of insulation and its thickness have a direct impact on the thermal performance of the panel. Rigid cellular foam is generally used as insulation, and the most common forms of this foam are extruded polystyrene (XPS) and expanded polystyrene.[1] Concrete wythes are connected to each other using tie connectors. These connectors are generally installed perpendicular to the face of the wall and carry mostly axial forces during handling[4,5] but provide very little composite action. To reach a higher level of composite action for enhanced structural performance, shear connectors are used to transfer the shear forces between concrete wythes. Traditional shear connectors, such as discrete concrete blocks or steel connectors, cause thermal bridging, significantly affecting the thermal performance of the wall. For example, using steel connectors with as low as an 0.08% reinforcement ratio can reduce the thermal performance of the panel by 38%.[6]

In service, most concrete insulated panels behave as a partially composite system due to the partial shear transfer and

relative end slip between wythes, though the panels initially behave as almost fully composite. The initial fully composite behavior is due to initial bond and friction between insulation and concrete, construction details, and the ties that hold the two wythes intact for handling purposes.[4,7–9] Determining the behavior of partially composite panels is a complex process that relies on experimental testing or a designer's experience. Several simplified methods have been proposed to assess the degree of composite action in these panels using experimental and theoretical parameters, including methods based on relative strength[1] and relative stiffness.[9,10] Pessiki et al.[9] investigated the effect of solid concrete regions on composite action and showed a higher shear transfer mechanism compared with other shear connector types. However, aside from causing thermal bridging, the concrete regions caused stress concentrations and premature flexural cracking of the panel. Hassan and Rizkalla[11] investigated commercially available carbon-fiber-reinforced polymer grids for shear transfer in sandwich panels and developed a method to calculate the partially composite moment capacity.

The facade wythe thickness usually ranges between 50 and 75 mm (2 and 3 in.) and is often governed by the concrete cover and fire resistance requirements.[1] Generally, the facade wythe is not designed to carry loads; however, it does contribute to the overall performance of the panel.[3,4,12,13] The thickness of the structural wythe ranges between 50 and 150 mm (2 and 6 in.) and its size is determined based on the applied loads and the level of composite action.[14,15] In the precast concrete industry, the costs of shipping, handling, and transporta-

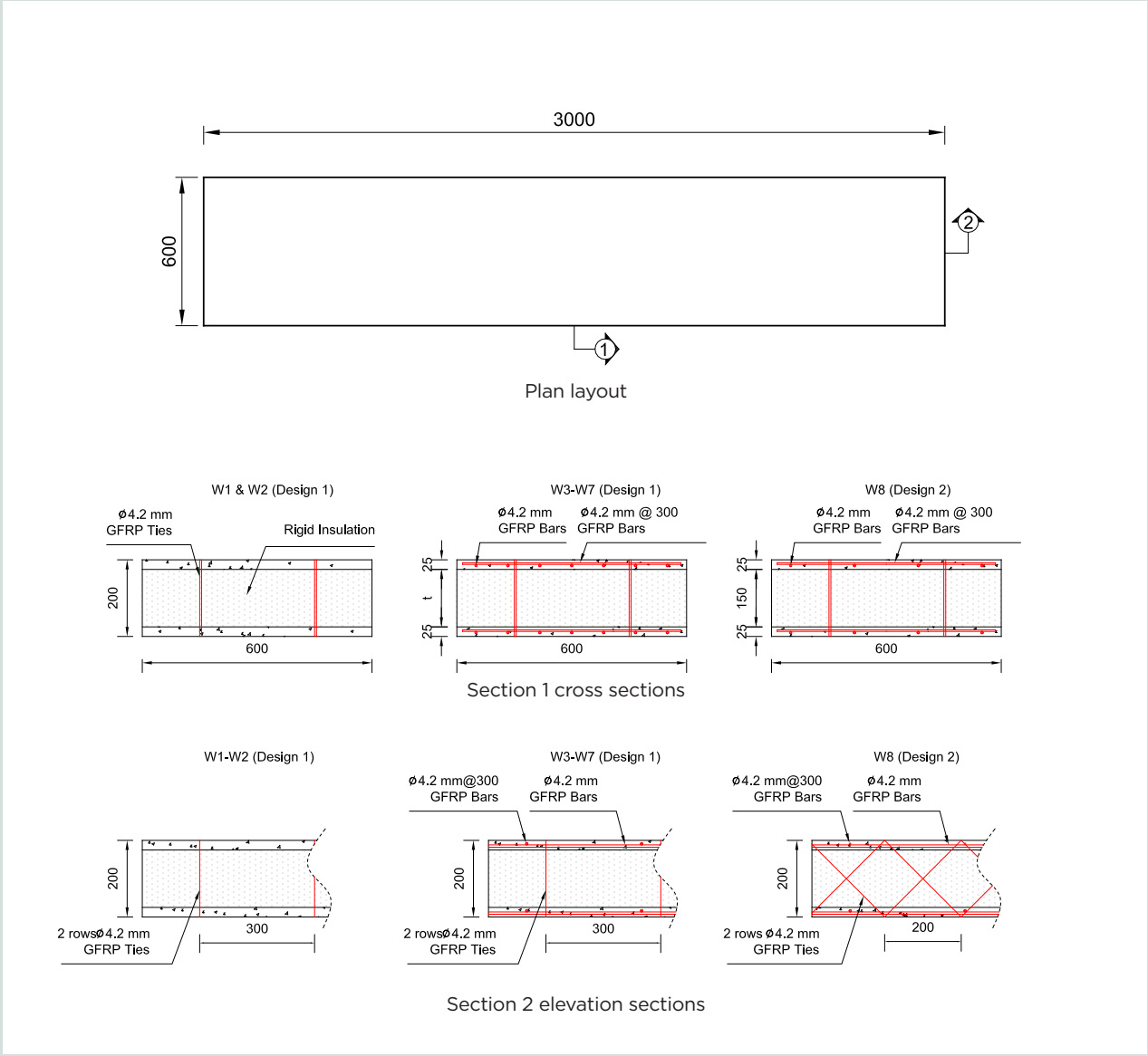


**Figure 1.** General panel configuration. Note: Dimensions are in millimeters. GFRP = glass-fiber-reinforced polymer; ⌀ = diameter. 1 mm = 0.0394 in.

tion are key parameters. As such, reducing the self-weight of precast concrete units is highly desired.

This study introduces a new design for insulated concrete walls using ultra-high-performance concrete (UHPC), which enables the fabrication of very thin wythes, only 25 mm (1 in.) thick, reducing self-weight significantly. The proposed wall design has a layer of XPS insulation and uses glass-fiber-reinforced polymer (GFRP) connectors. Previous studies have investigated the flexural performance of insulated walls using normal-strength concrete;[3,15,16] however, to the authors' knowledge, there are no published studies on UHPC insulated walls. This study explores the effect of different parameters on flexural strength: UHPC fiber type, namely steel compared with polyvinyl alcohol (PVA); insulation thickness; low and moderate composite action using transverse GFRP ties compared with diagonal GFRP connectors; and the use of GFRP flexural reinforcement to provide different reinforcement ratios in the wythes.

## Experimental study

Eight double-wythe precast UHPC insulated panels were fabricated and tested. All specimens were 3000 mm long by 600 mm wide (120 by 24 in.) with various overall thicknesses. The panels consisted of two 25 mm (1 in.) thick layers of concrete and a layer of XPS insulation sandwiched between the concrete wythes. The thickness of the insulation varied from 50 to 150 mm (2 to 6 in.) to simulate various thermal insulation requirements. To avoid the initial bond between the concrete and insulation, a thin layer of plastic was placed at the interface. GFRP reinforcement was used for this study. Two rows of 4.2 mm (0.17 in.) diameter GFRP ties spaced at 300 mm (12 in.) were used in seven specimens to connect the two wythes and represent a very low-composite-action design. Although such a design is not as structurally efficient as moderate- to high-composite-action designs, it is highly preferable when thermal bowing is a concern. One specimen was fabricated with diagonal GFRP connectors with an X pattern to develop a moderate level of composite action. **Figure 1** shows the typical plan layout and cross sections for all specimens. The following sections provide details of the experimental program, including materials, test matrix, fabrication, and test setup and instrumentation.

## Materials

**Ultra-high-performance concrete** A commercially available premixed concrete was used in this study with a very low water-to-cement ratio of approximately 0.2. Two types of fibers were explored in this study: steel and PVA. The steel fibers were 12 mm (0.5 in.) long with a tensile strength of 2750 MPa (400 ksi). The PVA fibers were also 12 mm long but with an 800 MPa (116 ksi) tensile strength. The material supplier recommended dosages for the fibers of 2% and 3% by volume for the steel and PVA fibers, respectively. The 2% dosage for steel fibers was recommended by the supplier, whereas the 3% for PVA was determined as the upper bound for workability based on trial batches. A total of 19 cylinders with PVA fibers and three with steel fibers were fabricated to determine the mechanical properties of the concrete in compression. The sixteen 100 × 200 mm (4 × 8 in.) and three 75 × 150 mm (3 × 6 in.) cylinders were demolded after four days and were exposed at room temperature until the day of the test. The cylinders were tested approximately three months after casting, and the average concrete compressive strength was 105 MPa (15.2 ksi) with a 6.9 MPa (1.00 ksi) standard deviation for the concrete with PVA fibers and 125 MPa (18.1 ksi) with a 10.6 MPa (1.54 ksi) standard deviation for the concrete with steel fibers. The modulus of elasticity was 34.5 GPa (5000 ksi) for cylinders with PVA fibers and 35.7 GPa (5180 ksi) for cylinders with steel fibers. The compressive strains recorded at the peak stresses were approximately 3980 microstrains for the cylinders with PVA fibers and 3608 microstrains for the cylinders with steel fibers.

The flexural strength of concrete was evaluated using the third-point loading test method. Nine 50 × 100 × 400 mm (2 × 4 × 16 in.) prisms and three 75 × 75 × 300 mm (3 × 3 × 12 in.) prisms were tested with PVA fibers, and three 50 × 100 × 400 mm (2 × 4 × 16 in.) prisms were tested with steel fibers. Researchers[17,18] have shown that this method overestimates the tensile cracking strength of concrete because it cannot accurately predict the postcracking behavior of concrete due to the presence of the fibers. The concrete will exhibit extensive cracking prior to failure, and therefore, the concrete prism will no longer behave elastically along its depth. A correction factor to account for the overestimation of the tensile cracking strength based on the third-point bending test was proposed by the Association Française de Génie Civil[19] to calculate the actual strength $f_{ct}$ from the measured strength $f_{ct,flexure}$ using Eq. (1). The reference depth $d_0$ is set to 100 mm (4 in.) based on the experimental tests, and the actual depth of the specimen is $d$.

$$f_{ct} = f_{ct,flexure}\left(\frac{2.0\left(\frac{d}{d_0}\right)^{0.7}}{1+2.0\left(\frac{d}{d_0}\right)^{0.7}}\right) \quad (1)$$

The flexural strengths based on the peak loads from the prism tests, before applying the correction factor, for concrete reinforced with PVA and steel fibers were 16 and 27 MPa (2.3 and 3.9 ksi), respectively. The flexural strength based on the first cracking load was around 54% of the peak load strength, namely, 8.6 MPa (1.2 ksi) for concrete with PVA fibers and 14.6 MPa (2.1 ksi) for concrete with steel fibers. The correction factor based on the 100 mm (4 in.) deep prisms is 66%. Using this correction factor, the calculated tensile strengths of concrete are 5.5 MPa (0.80 ksi) for concrete with PVA fibers and 9.5 MPa (1.4 ksi) for concrete with steel fibers. Similar results were reported by other authors for concrete with steel fibers using the same correction factors.[18]

The tensile strength of concrete was also measured using the standard method for splitting cylinders per ASTM C496.[20]

Split tests on four cylinders showed concrete tensile strengths of 12.85 MPa (1.86 ksi) for concrete with PVA fibers based on peak load. It was reported that the direct tensile strength is approximately 35% of the strength from the split test using the peak load,[18] and therefore the tensile strength for concrete with PVA fibers was 4.5 MPa (0.65 ksi). Similar results for the direct tensile strength of concrete reinforced with PVA fibers were reported by Meng et al.[21] The direct tensile strength of UHPC reinforced with steel fibers was assumed to be 6.2 MPa (0.90 ksi), which is 5% of the concrete's compressive strength, a proposed ratio from the report by the Federal Highway Administration[18] on UHPC material testing.

**GFRP reinforcement** The panels for this study were reinforced with 4.2 mm (0.17 in.) diameter GFRP sand-coated reinforcing bars. The flexural reinforcement grid was assembled using individual reinforcing bars connected with small zip ties. The connector ties were cut to the exact length such that they were fully embedded in each concrete wythe. The ends of these ties were sharpened to generate a pointed end for ease of insertion through the insulation layer and so they would not appear on the outer surface of the wythe after fabrication. The diagonal connectors were glued with structural epoxy to form the X-shaped shear grid. The nominal tensile strength of the GFRP reinforcing bars provided by the supplier was 1050 MPa (152 ksi). The tensile modulus was 45.2 GPa (6560 ksi), and the transverse shear strength was 212 MPa (30.7 ksi).

## Test matrix

**Table 1** shows the test matrix and parameters investigated in this study. The first two panels, W1 and W2 (Fig. 1), were used to investigate the effect of fiber type, either steel or PVA, and were fabricated without the additional GFRP flexural reinforcement. To assess the effect of increasing the GFRP flexural reinforcement ratio, specimen W2, which contained no reinforcing bars, was used as a control specimen to compare with specimens W3, W4, and W7 (Fig. 1) with reinforcement ratios ranging from 0.28% to 0.92%. Specimens W5 and W6 (Fig. 1) were compared with specimen W3 to assess the effect of the XPS insulation thickness ranging from 50 to 150 mm (2 to 6 in.). The effect of the wythe connectors was evaluated by comparing specimens W3 to W7 with transverse ties of 0.0145% reinforcement ratio (relative to surface area) with specimen W8 with diagonal X-shaped connectors of 0.048% reinforcement ratio (Fig. 1).

## Fabrication of specimens

Before the concrete was cast, the foam insulation boards were cut to size and wrapped with a plastic sheet to act as a bond breaker, thereby preventing any initial adhesion between the concrete and the insulation. The wythe connectors were then inserted through the insulation boards with an overhang of 25 mm (1 in.) for embedment in concrete on either side of the insulation. All panels were cast horizontally on formwork made of vinyl-faced plywood sheets for a smooth finish. The bottom wythe was cast first. The concrete was placed gradually in a back-and-forth motion to ensure that the fibers were oriented in the longitudinal direction of the panel. The insulation board assembly was then inserted immediately after casting the bottom wythe, and the seam between the insulation and the formwork was sealed to prevent any leakage of the concrete, which could cause uplift of the insulation. The top wythe was then cast three to four hours after the bottom wythe.

A plastic sheet was placed on top of the fresh concrete immediately after casting as recommended by the concrete supplier. The specimens were demolded three to four days after casting and were left at room temperature until the day of testing. Although the concrete supplier recommended that specimens should be moist cured for at least seven days, the specimens were not moist cured because this provided a more realistic representation of common production practices in the precast concrete industry. **Figure 2** shows the fabrication process for the panels.

**Table 1.** Test matrix

| ID | Connector type | Insulation thickness, mm | Longitudinal reinforcing bars per wythe | Longitudinal reinforcement ratio of cross-sectional area, % | Connector reinforcement ratio of surface area, % | Fiber type |
|---|---|---|---|---|---|---|
| W1 | Vertical | 150 | 0 | 0.0 | 0.0145 | Steel |
| W2 | Vertical | 150 | 0 | 0.0 | 0.0145 | PVA |
| W3 | Vertical | 150 | 7 | 0.64 | 0.0145 | PVA |
| W4 | Vertical | 150 | 3 | 0.28 | 0.0145 | PVA |
| W5 | Vertical | 50 | 7 | 0.64 | 0.0145 | PVA |
| W6 | Vertical | 100 | 7 | 0.64 | 0.0145 | PVA |
| W7 | Vertical | 150 | 10 | 0.92 | 0.0145 | PVA |
| W8 | ±45° | 150 | 4 | 0.37 | 0.0480 | PVA |

Note: ID = identifier; PVA = polyvinyl alcohol. 1 mm = 0.0394 in.

Formwork

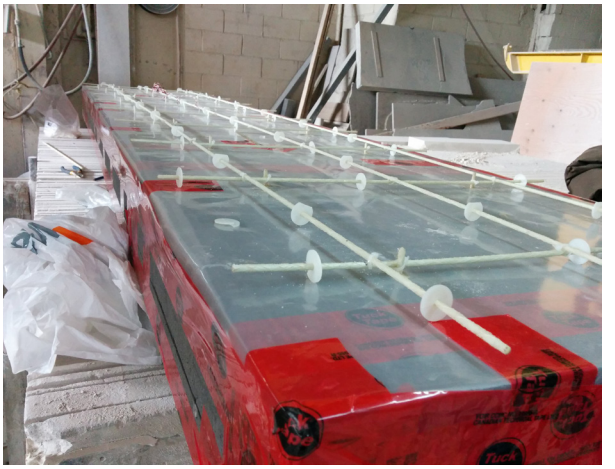

Assembling the insulation boards and GFRP reinforcement

Placing the UHPC

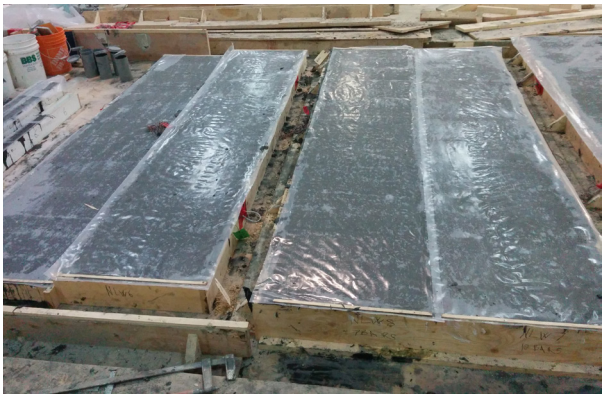

Freshly placed concrete covered with plastic

**Figure 2.** Fabrication of UHPC insulated panels. Note: GFRP = glass-fiber-reinforced polymer; UHPC = ultra-high-performance concrete.

## Test setup and instrumentation

The specimens were tested horizontally in a four-point bending configuration. The specimens were supported by a pin at 75 mm (3 in.) from one end and a roller at 75 mm from the other end, giving a structural span of 2850 mm (112 in.). Two point loads were applied at the third points of the span, giving a constant moment zone of 950 mm (37 in.). Panels in practice are loaded by wind while in a vertical position, and their self-weight does not induce flexure. To account for the difference between the configuration of the panels in practice compared with the testing configuration, once the test panel was placed horizontally in position over the supports, it was jacked up using a spreader beam to bring it to a level position and remove any sag due to the 2.2 kN (0.49 kip) calculated self-weight of the panel and steel spreader beams. The jacking was then released gradually and deflections were measured until the panel came back to its original deflected position.

Testing was conducted using stroke control at a rate of 2 mm (0.08 in.) per minute initially, which was increased to 5 mm (0.2 in.) per minute due to excessive deflection as the panels approached their ultimate capacity.

Deflection at midspan of the panel was measured using a 100 mm (4 in.) linear potentiometer (LP). Two LPs were used to measure the relative end slip between concrete wythes at each end. Two 30 mm (1.2 in.) long electric resistance strain gauges were used to measure the strains at the midspan of the panel at two levels within each 25 mm (1 in.) thick concrete wythe. **Figure 3** shows the instrumentation and test setup configuration for a typical panel.

## Experimental results

The results from the experimental testing of the eight UHPC insulated panels are presented in this section.

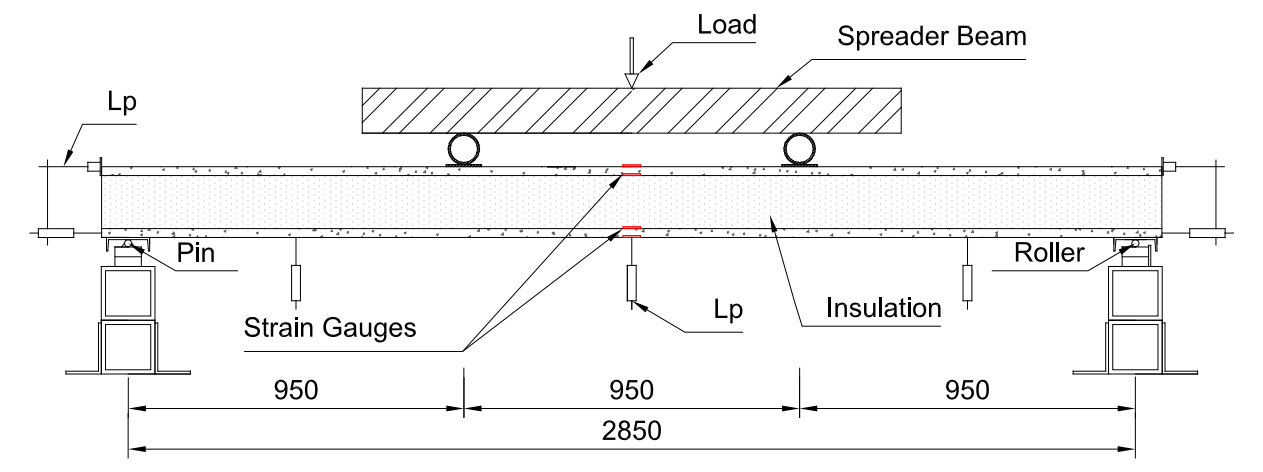


**Figure 3.** Typical test setup configuration and instrumentation. Note: Dimensions are in millimeters. Lp = linear potentiometer. 1 mm = 0.0394 in.

**Tables 2** and **3** present a summary of key test results. A comparison among specimens with different parameters was made in terms of the load–deflection, load–end slip, and load–strain responses for each panel. As mentioned previously, the specimens were jacked up to reach a leveled position along their span prior to applying any transverse test loads. Then, the jacking was released slowly until the panel gradually reached its original deflected position. This deflection was recorded and is shown in Table 2 as the initial deflection. The equivalent point load of 2.2 kN (0.49 kip) for the panel and spreader beam self-weights and the corresponding initial deflections were then accounted for in the measured test results.

## Load-deflection responses

**Figure 4** shows the load-deflection responses for all test specimens. For specimens W1 to W7 with low composite action, the response was trilinear, with an initial stiff response prior to full cracking followed by a lower stiffness response after cracking and excessive slip leading to loss of composite action. Then, the third region interestingly showed an

**Table 2.** Summary of test results

| ID | Initial deflection, mm | Deflection at ultimate load, mm | Ultimate load, kN | Ultimate NC* load, kN | Ultimate NC† load, kN | Ultimate FC‡ load, kN | Composite action, % | Service load, kN |
|---|---|---|---|---|---|---|---|---|
| W1 | 10.2 | 212 | 10.9 | 2.1 | 5.1 | 42.0 | 15 | 1.7 |
| W2 | 17.1 | 150 | 5.2 | 2.1 | 3.0 | 30.0 | 8 | 1.0 |
| W3 | 32.9 | 194 | 9.2 | 4.5 | 5.0 | 52.0 | 9 | 0.5 |
| W4 | 14.9 | 212 | 9.8 | 3.2 | 4.2 | 40.0 | 15 | 1.2 |
| W5 | 50.0 | 258 | 3.9 | 4.5 | 4.2 | 25.0 | 0§ | 0.3 |
| W6 | 23.4 | 187 | 6.0 | 4.5 | 4.2 | 38.0 | 5 | 0.7 |
| W7 | 15.8 | 192 | 8.8 | 5.5 | 5.8 | 61.0 | 5 | 1.1 |
| W8 | 0.0 | 47 | 17.3 | n.d. | 4.21 | 45.0 | 32 | 12.1 |

Note: FC = fully composite; ID = identifier; NC = noncomposite; n.d. = no data available. 1 mm = 0.0394 in.; 1 kN = 0.225 kip.

* NC value from experimental testing of small-scale single wythes. The load was then scaled up from the moment to take into account the length and the second wythe of the full-scale testing.

† NC value from Response2000 and theoretical calculations.

‡ FC value from Response2000 and theoretical calculations.

§ Assumed to have zero composite action. A variation of thickness by even 2 mm would reduce the theoretical NC load below the ultimate test load.

**Table 3.** Total end slip at service and ultimate loads

| ID | End slip at service load, mm | End slip at ultimate load, mm | Ultimate load, kN |
|---|---|---|---|
| W1 | 2.7 | 67.1 | 10.9 |
| W2 | 2.5 | 45.8 | 5.2 |
| W3 | 2.5 | 67.3 | 9.2 |
| W4 | 2.7 | 70.0 | 9.8 |
| W5 | 1.1 | 37.1 | 3.9 |
| W6 | 1.8 | 39.1 | 6.0 |
| W7 | 2.6 | 64.9 | 8.8 |
| W8 | 1.9 | 5.7 | 17.3 |

Note: ID = identifier. 1 mm = 0.0394 in.; 1 kN = 0.225 kip.

increased stiffness response. It is hypothesized that as end slip increases between wythes, the GFRP ties, which are originally vertical and have zero tension, start rotating to a diagonal position to accommodate the relative slip. As such, the ties elongate, thereby developing a tension force (that is, self-stressing). The horizontal component of the diagonal tension resists the relative slip and slows down its progress, which stabilizes the composite action and leads to the apparent stiffening.

## Performance relative to service load requirements

The performance was assessed in terms of strength and serviceability requirements, including service load based on wind loading, permissible deflection limit, and permissible GFRP stress limit. The concrete stress level was also checked. The calculated equivalent service wind load was 0.95 kN (0.21 kip), which is based on a three-story building in Toronto, ON, Canada, subjected to 0.74 kPa (0.11 psi) wind pressure. The deflection limit was set to the span divided by 360, which is 7.9 mm (0.31 in.). The stress limit for GFRP reinforcement according to the Canadian Standards Association S806-12[22] is 25% of the reported tensile strength. In all test panels, the service loads were governed by the deflection criteria, not the GFRP stress limit, and are reported in Table 2. The concrete compressive stress was monitored at the service loads and ranged from 3.7 to 6.6 MPa (0.54 to 0.96 ksi) for the different specimens, which was only 3% to 6% of the ultimate compressive strength. Specimens W1, W2, W4, W7, and W8 reached service loads (at the deflection limit of 7.9 mm) greater than the calculated service wind load of 0.95 kN.

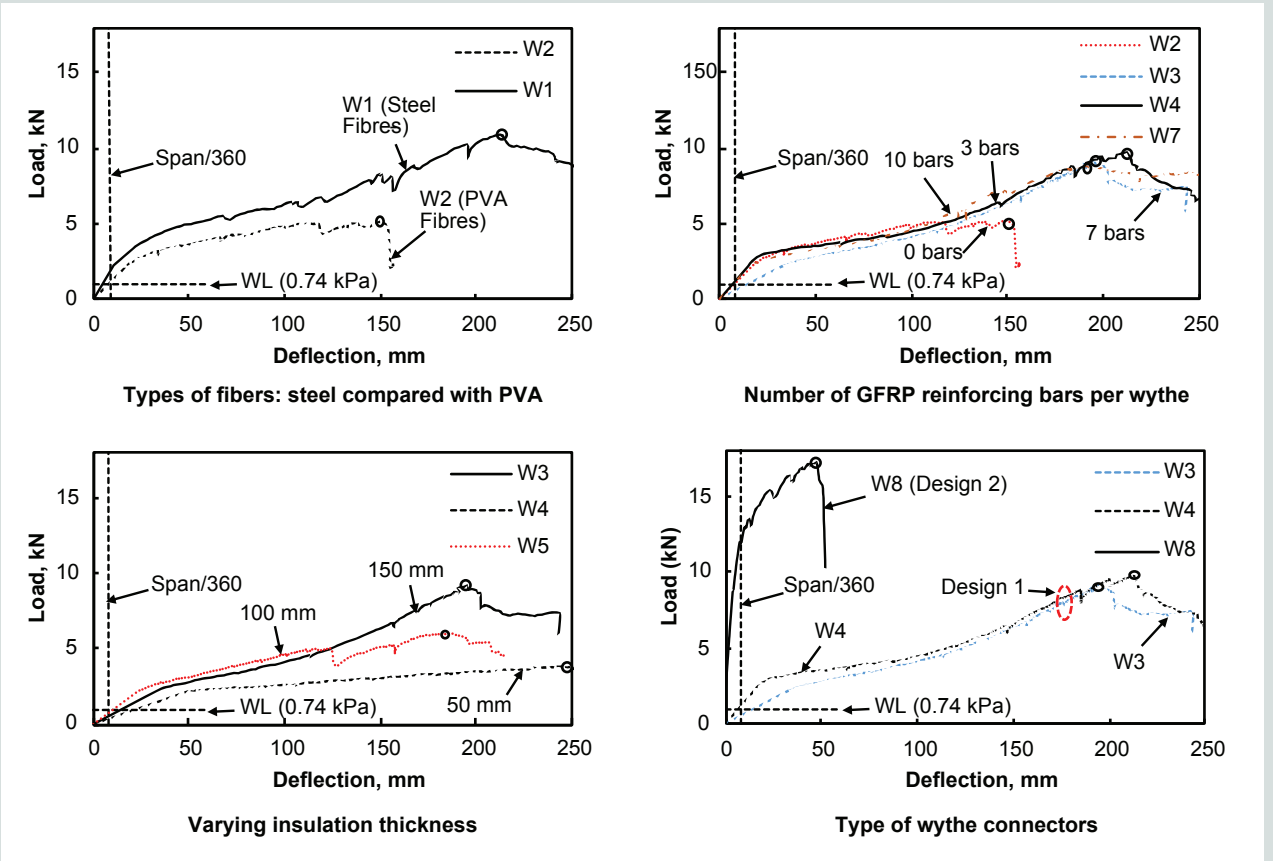


**Figure 4.** Load–deflection responses. Note: GFRP = glass-fiber-reinforced polymer; o = ultimate load reached; PVA = polyvinyl alcohol; WL = wind load. 1 mm = 0.0394 in.; 1 kN = 0.225 kip; 1 kPa = 0.145 psi.

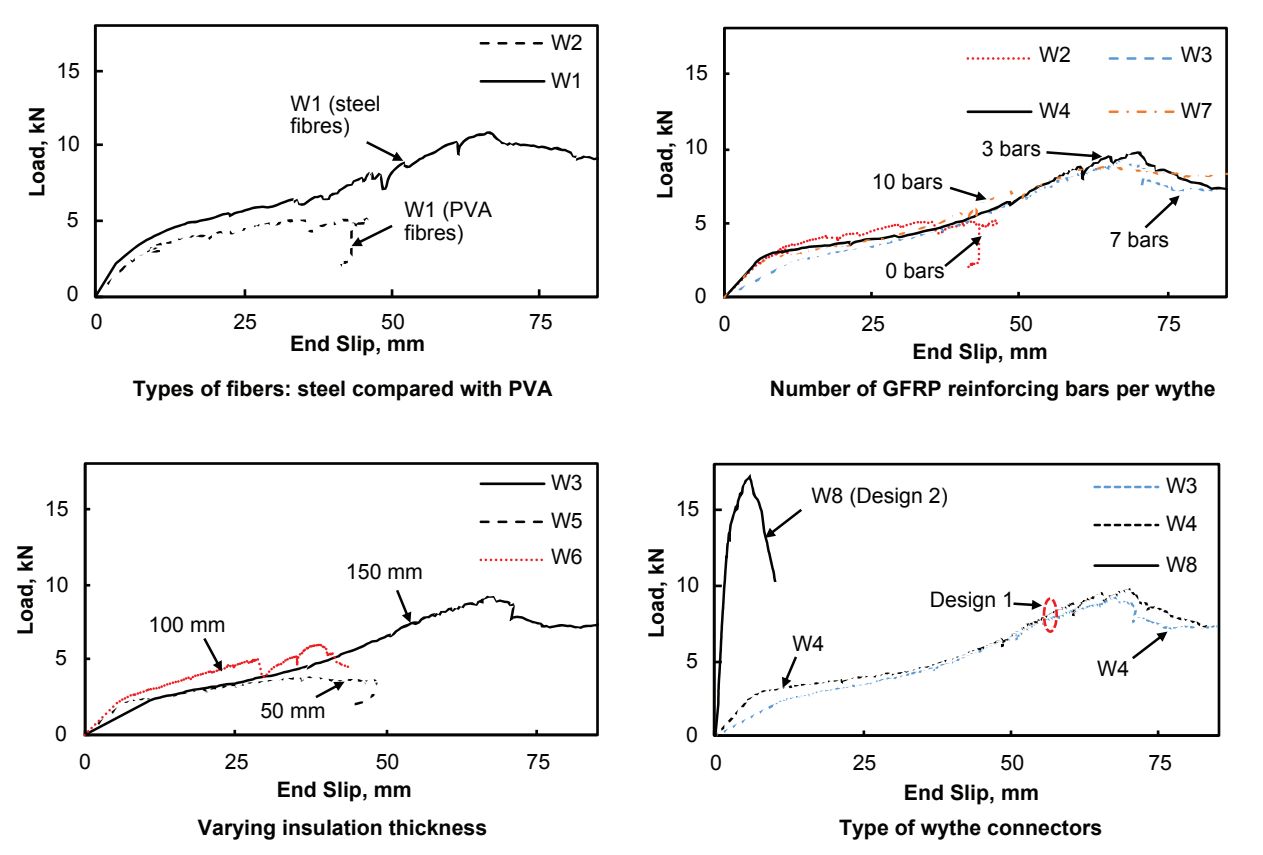


**Figure 5.** Load–total end slip responses. Note: GFRP = glass-fiber-reinforced polymer; PVA = polyvinyl alcohol. 1 mm = 0.0394 in.; 1 kN = 0.225 kip.

Specimens W3, W5, and W6 did not satisfy the wind load requirement at the permissible deflection limit.

## Load–end slip responses

**Figure 5** shows the load–end slip responses for all specimens. The relative end slip was measured on each end of the panel using a 100 mm (4 in.) LP with its base fixed on one wythe while measuring the relative slip on the other wythe. The cumulative slip from both ends of the panel was then added and plotted against the total transverse load applied. Once the transverse load was applied, the end slip was noticeable and continued to increase for specimens W1 to W7, indicating very low levels of composite action, especially because there was no bond between the concrete and insulation. An excessive amount of slip was measured in these specimens at ultimate. The cumulative end slip for specimen W8 was much less than the other specimens (Fig. 5), indicating a higher degree of composite action. The amount of end slip for each specimen at the service and ultimate loads is reported in Table 3.

## Load–strain responses

**Figure 6** shows the load–strain responses at midspan for each specimen, including the top wythe strain and bottom wythe strains. Strain readings were greatly affected by the cracks developing near the gauge area during the tests. Each wythe experienced extreme fiber compressive and tensile strains, suggesting that each wythe had its own neutral axis as a result of the relatively low composite action. The maximum compressive strain in any wythe did not exceed -3500 microstrains, which is below the -3980 microstrains reported at peak compressive strength from the cylinder testing.

**Figure 7** shows the strain profiles for each specimen at its service and ultimate state. The strain readings for specimens W2, W4, and W8 were greatly affected by a major crack that developed outside of the constant moment zone of the top wythe.

## Effect of fiber type

Two types of fibers, steel and PVA, were used in the concrete. As explained earlier, the tensile strength of concrete was greatly affected by the type of fiber, resulting in approximately 60% higher strength with steel fibers compared with PVA fibers, whereas the compressive strength was only 19% higher for the concrete with the steel fibers. The effect of the fiber type on the structural performance of the panel can be assessed by comparing specimens W1 (steel fibers) with W2 (PVA fibers), both without any internal reinforcing bar and with 150 mm (6 in.) thick insulation (Fig. 4–6).

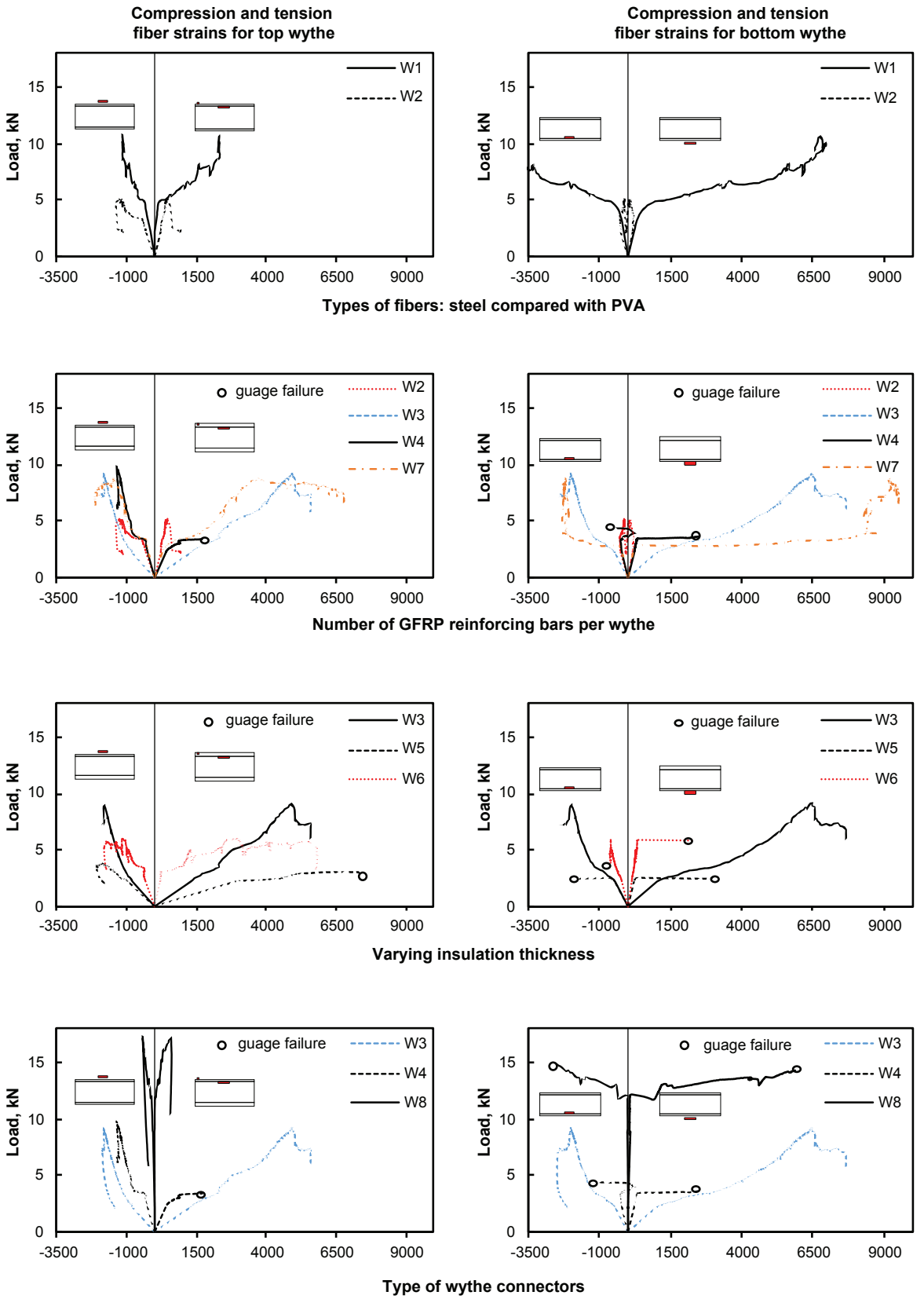


**Figure 6.** Load–strain responses. Note: GFRP = glass-fiber-reinforced polymer; PVA = polyvinyl alcohol. X-axes are in units of microstrain. 1 kN = 0.225 kip.

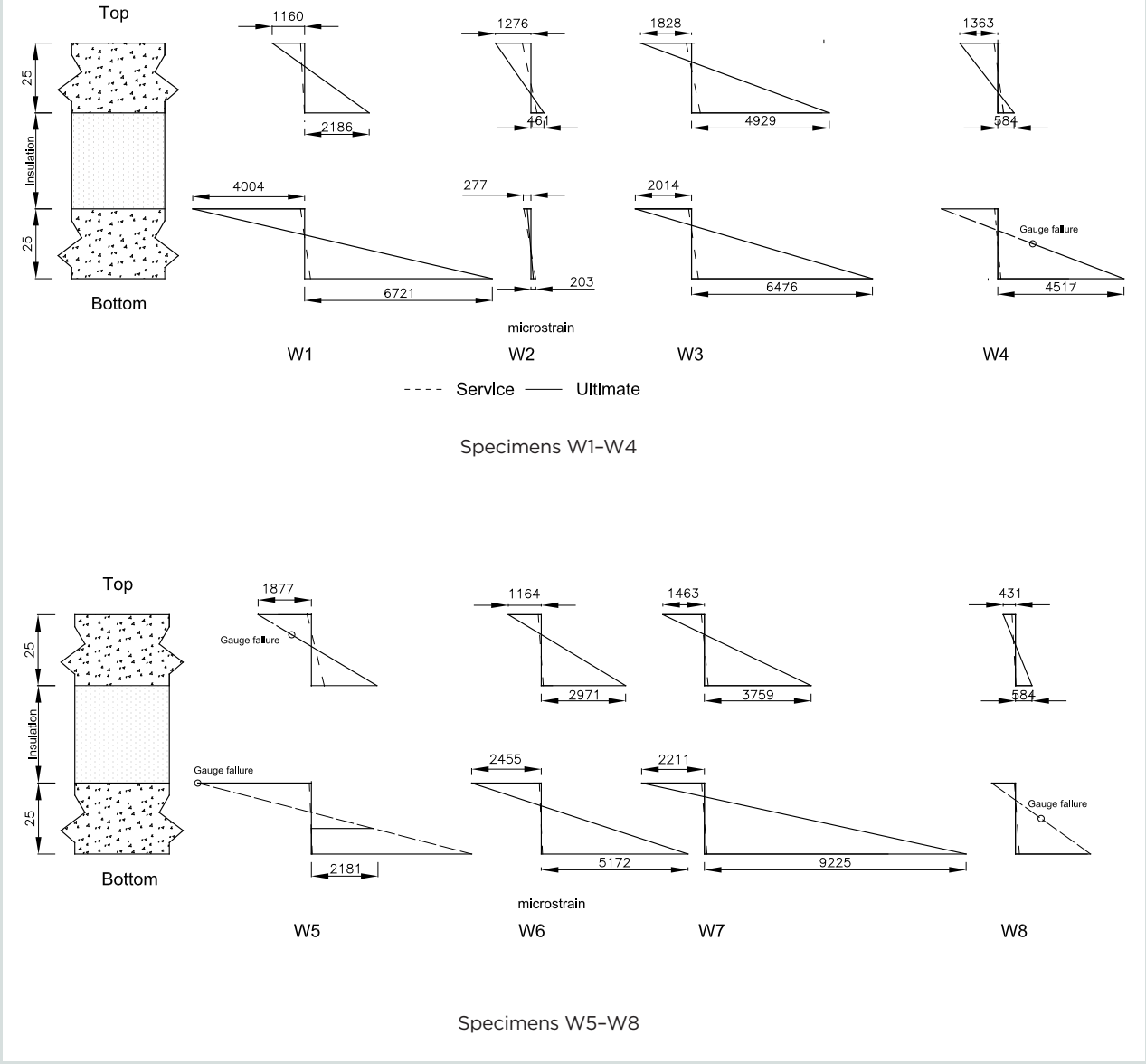


**Figure 7.** Strain profiles at service and ultimate loads. Note: Units are in microstrain.

Specimen W1 reached 2.1 times the strength of W2 and was also stiffer. For example, at the peak load of W2, its deflection was 2.4 times that of W1 at the same load level. Similarly, the total end slip of W2 was 2.4 times that of W1 at the same load.

## Effect of reinforcement ratio

The effect of the reinforcement ratio on the structural performance of the panel can be assessed by comparing specimens with different reinforcement ratios as follows: W2 (no reinforcing bars, 0%), W4 (three reinforcing bars, 0.28%), W3 (seven reinforcing bars, 0.64%), and W7 (10 reinforcing bars, 0.92%), all with PVA fibers and 150 mm (6 in.) thick insulation (Fig. 4–6). Adding longitudinal GFRP reinforcing bars resulted in a noticeable increase in ultimate load, ranging from a 69% to a 88% increase compared with the specimen with no longitudinal reinforcing bars, with no direct correlation to reinforcement ratio. In fact, the lowest ratio (W4) resulted in the highest ultimate load gain of 88%. The lack of correlation to reinforcement ratio is attributed to the failure mode as well as the proximity of the reinforcing bar to the neutral axis within each wythe. It is also interesting to note that W4, with a GFRP reinforcement ratio

of 0.28% and PVA fibers, reached a comparable ultimate strength to W1 with no reinforcing bars but with steel fibers (the ultimate strength of W4 was only 10% lower than W1). However, unlike steel fibers, the GFRP reinforcing bars did not affect stiffness or relative slip at all, regardless of reinforcement ratio.

## Effect of insulation thickness

The effect of insulation thickness on the performance of the panels can be assessed by comparing specimens W5 (50 mm [2 in.] insulation thickness), W6 (100 mm [4 in.] insulation thickness), and W3 (150 mm [6 in.] insulation thickness), all with seven GFRP reinforcing bars and PVA fibers (Fig. 4–6). A fully noncomposite thin panel theoretically should not be affected by its insulation thickness. However, because some low levels of composite action were reached, the insulation thickness had an impact on the ultimate capacity of the panel. Reducing the insulation thickness by 33% (from 150 to 100 mm [6 to 4 in.]) resulted in a 35% reduction in ultimate strength, while reducing it by 67% (from 150 to 50 mm [6 to 2 in.]) resulted in a 58% reduction in ultimate strength. The end slip at the same load level was not affected much by the insulation thickness.

## Effect of shear connectors

As explained previously, specimens W1 to W7 were designed as a low-level composite system and were fabricated with transverse GFRP ties (design 1 in Fig. 1) of 0.0145% reinforcement ratio, whereas specimen W8 was designed to achieve a moderate degree of composite action and was fabricated using a diagonal X-shaped assembly of GFRP connectors (design 2 in Fig. 1) of 0.048% reinforcement ratio. The effect of this parameter on the response is illustrated in Fig. 4 to 6, which compares W4 and W3 with W8. It was established earlier that flexural reinforcement ratio had very little impact on ultimate capacity and stiffness. As such, the slight differences in reinforcement ratios between W8 and the other two specimens should not have much effect. The effect of the angled connectors (design 2) on the overall structural performance was remarkable. The ultimate strength increased by 82% with diagonal connectors compared with the average ultimate strength of the specimens with transverse ties, but perhaps the most significant impact was on stiffness and slip. At a load equal to the average ultimate capacities of W3 and W8, the deflection and slip of W8 were less than 4% of the result for the other two panels. While Fig. 6 suggests that both wythes still had their respective neutral axes in W8 based on strain responses, the strain magnitudes in the upper wythe were significantly lower than in the bottom wythe, unlike the strain response of the other two panels.

## Degree of composite action

The PCI Precast Sandwich Wall Panels Committee[1] presents a method to evaluate the degree of composite action $K_u$ in sandwich panels as follows:

$$K_u = \frac{M_u - M_{u,NC}}{M_{u,FC} - M_{u,NC}} \times 100 \quad (2)$$

where

$M_u$ = experimentally measured ultimate moment of the partially composite panel

$M_{u,NC}$ = theoretical ultimate moment for the noncomposite case of the same panel

$M_{u,FC}$ = theoretical ultimate moment for the fully composite case of the same panel

The values of $M_{u,NC}$ and $M_{u,FC}$ were predicted theoretically using the computer program Response2000,[23] which is based on the concepts for equilibrium, strain compatibility, and the material constitutive relationships through cracked section analysis. For the noncomposite case, a single wythe was analyzed with Response2000 and the ultimate moment was multiplied by two to get $M_{u,NC}$. Small sections (720 mm [28 in.] long) of a single wythe were also cut from the end of the specimens and tested experimentally to assess the ultimate loads of the noncomposite system. The results from both methods are reported in Table 2.

The model developed by researchers at the Federal Highway Administration[18] is adopted in this study to represent the stress-strain response of UHPC in compression. A bilinear model for tension was used, with a peak strength of 6.2 and 4.5 MPa (0.90 and 0.65 ksi) for steel and PVA fibers, respectively, and ultimate strains of 2.8% and 4% for PVA and steel fibers, respectively.[18,21]

**Figure 8** shows the experimental load–deflection curves along with the calculated load–deflection curves for the noncomposite and fully composite cases for each specimen. Using Eq. (2), the degree of composite action was calculated for all specimens. Specimens W1 to W7 experienced 5% to 15% composite action, excluding W5. Specimen W5 reached a load slightly lower than the theoretical noncomposite load, which may be due to a variation of the actual wythe thickness, which varied along the span between 22 and 27 mm (0.87 and 1.1 in.). Specimen W8, alternatively, reached 32% composite action as a result of the more effective GFRP shear connector design.

## Cracking behavior

Based on the theoretical elastic calculations, the cracking loads for a single wythe are 0.65 and 0.86 kN (0.15 and 0.20 kip) for the PVA and steel fibers, respectively. Assuming noncomposite behavior (which is a reasonable assumption for specimens W1 to W7), this translates into approximate cracking loads of 1.3 and 1.72 kN (0.30 and 0.39 kip) for the double-wythe panels. For the fully composite case, the calculated cracking loads are 22 and 30 kN (4.9 and 6.7 kip) for PVA and steel fibers, respectively. The self-weight of the

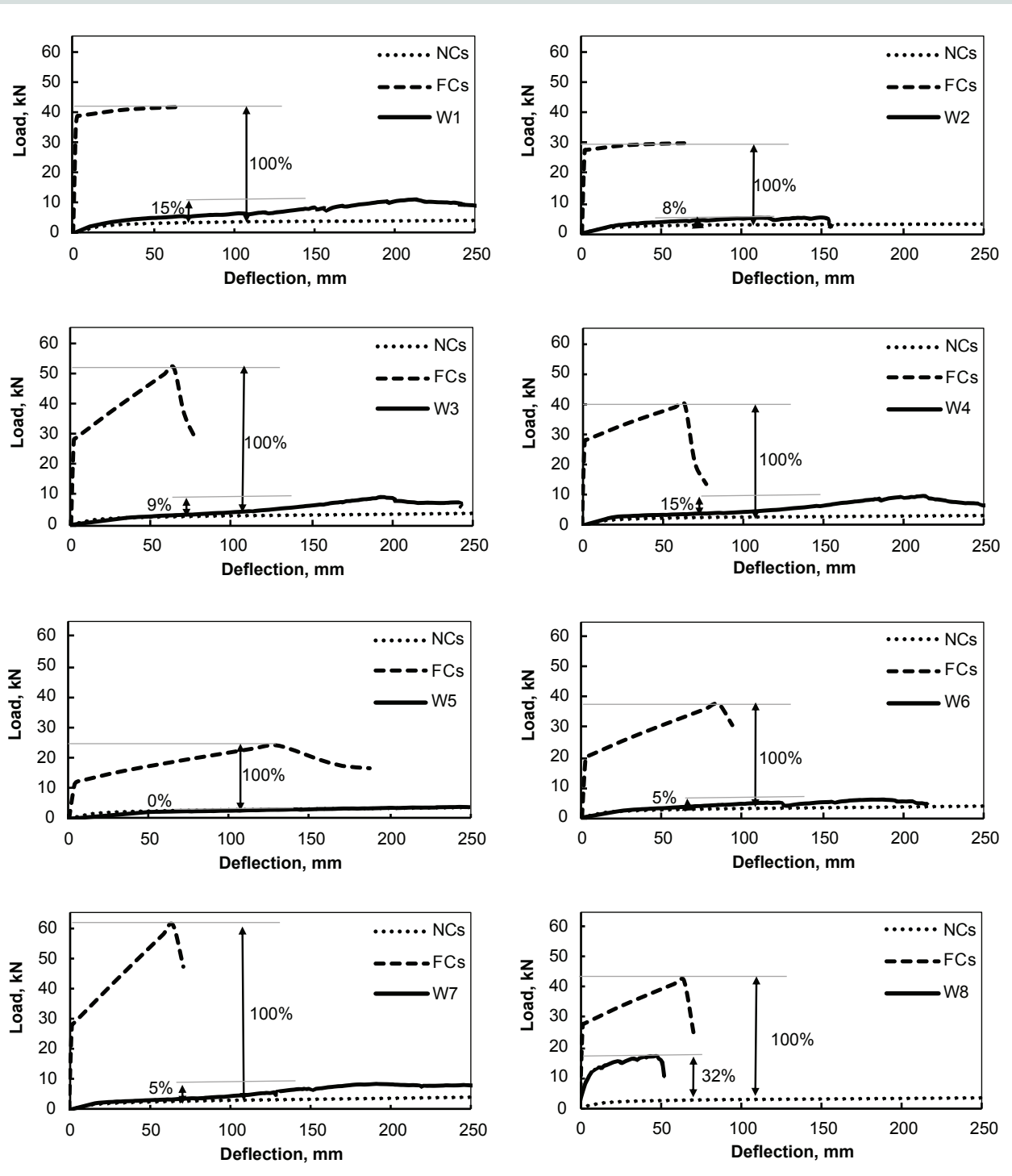


**Figure 8.** Level of composite action. Note: Solid lines represent experimental results; dashed lines represent theoretical results. FCs = fully composite systems; NCs = noncomposite systems. 1 mm = 0.0394 in.; 1 kN = 0.225 kip.

panel and spreader beams (2.2 kN [0.49 kip]) is higher than the cracking load (assuming a completely noncomposite panel). This explains the few cracks (typically one to three hairline cracks) that were observed under self-weight in W1 to W7 before applying loads. Alternatively, a clear cracking event was observed for W8 during the test at 8.9 kN (2.0 kip), indicating that this specimen experienced a higher level of composite action throughout the test compared with specimens W1 to W7; however, more cracks developed. **Figure 9** shows the cracking patterns of specimens W1, W2, and W3 mapped after the test. Each panel had a distinct crack pattern. W3 was selected as a sample, but the crack patterns for W4 to

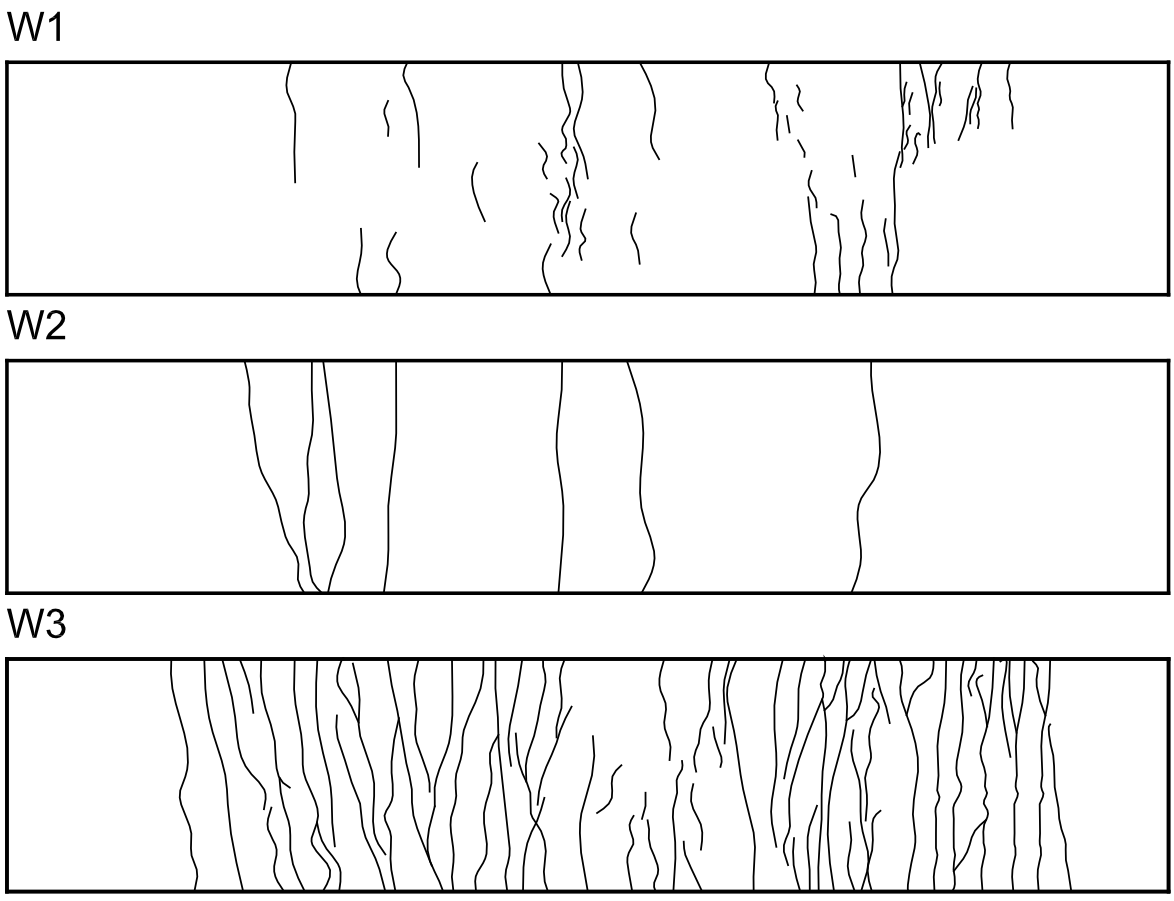


**Figure 9.** Cracking patterns after the test (underside of bottom wythe).

W8 were similar. W1 and W2 showed fewer cracks compared with W3. Fewer continuous cracks developed in W2 with PVA fibers relative to a larger number of discontinuous cracks that developed in W1 with steel fibers. W3 to W8, alternatively, developed a very dense network of continuous cracks as a result of the GFRP reinforcing bars.

## Failure modes

The primary failure mode of specimens W1 to W7 was fracture of the GFRP ties at the interface with the concrete wythe. The top row of **Fig. 10** shows the specimen W1 with the insulation removed after the test. No pull-out bond failure occurred despite the short (25 mm [1 in.]) embedment of the ties. As the top wythe slips longitudinally relative to the bottom wythe, the GFRP ties are forced into a diagonal orientation, which implies elongation of the ties and development of a tension force. Based on the mechanical properties of the connectors, it was estimated that a 30 mm (1.2 in.) relative slip between wythes would result in the connector reaching its ultimate state. The load–end slip graphs (Fig. 5) show that most of the specimens exceeded the 30 mm end slip at each end of the panel. In addition, as the relative slip progressed, a bend formed in the reinforcing bar at the interface of the concrete wythe with the insulation (Fig. 10). The combination of tension and a bend in the reinforcing bar caused the ties to fail. For specimen W8, the primary failure mode occurred by failure of the diagonal GFRP ties, including both compression and tension failures within the X pattern (Fig. 10). The connectors started to fail from the end and progressed toward the middle of the panel. Each drop in the load–deflection curve (Fig. 4) prior to the ultimate failure indicates a connector failure.

Additional secondary failure modes occurred in the specimens. In W1, W4, and W8, a separation occurred between the top wythe and insulation (Fig. 10). In W1 and W2 (without longitudinal reinforcing bars), a major flexural crack also developed in the bottom wythe, and eventually the wythe fractured at the crack location (Fig. 10). In specimens W3 and W5 to W7, the test was stopped after the load declined sufficiently due to excessive deflection (Fig. 3).

Fracture of GFRP ties near the concrete face in W1 to W7

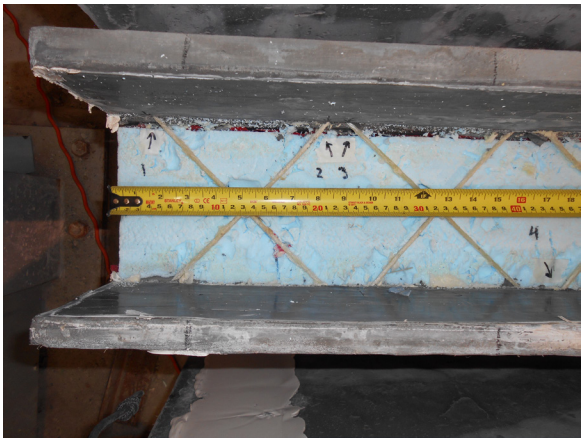

Failure of the diagonal GFRP connectors in W8, some in tension and some in compression

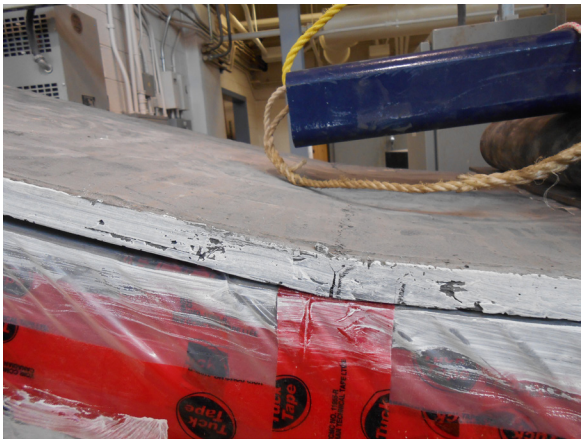

Major separation of the top wythe of W1 and W8

Major crack of the bottom wythe in W2 and W3

**Figure 10.** Failure modes. Note: GFRP = glass-fiber-reinforced polymer.

## Conclusion

In this study, new designs of double-wythe insulated wall panels using UHPC were investigated, namely a low-composite system with GFRP transverse ties and a moderately composite system with X-pattern GFRP connectors. Very thin 25 mm (1 in.) wythes were used to reduce self-weight significantly. A UHPC panel with PVA fibers was compared with a panel with steel fibers. The XPS insulation thickness was varied from 50 to 150 mm (2 to 6 in.) and GFRP longitudinal flexural reinforcement in the wythes was varied from 0% to 0.92% reinforcement ratio. All specimens were cast horizontally and completed the same day, then air cured at room temperature. The following conclusions were drawn from the study:

- When comparing the panels without GFRP flexural reinforcement, the panel with steel fibers reached more than twice the strength of the panel with PVA fibers. The panel with steel fibers was also significantly stiffer. Its deflection and relative slip between wythes were both about 40% of those for the panel with PVA fibers. At the UHPC material level, the compressive and tensile strengths with steel fibers were 19% and 56%, respectively, higher than with PVA fibers.

- Adding flexural GFRP reinforcement to the wythes generally resulted in a noticeable increase of ultimate load, ranging from a 69% to 88% increase compared with the specimen no flexural reinforcement, but the increase had no rational correlation to the reinforcement ratio, which varied from 0.28% to 0.92%. This lack of correlation is attributed to the failure mode and the proximity of the reinforcing bars to the neutral axis within each wythe.

- The panel with 0.28% GFRP reinforcement ratio and PVA fibers reached an ultimate strength (only 10% lower) comparable to that of the panel with steel fibers but no GFRP reinforcing bar. However, unlike steel fibers, the GFRP reinforcing bar did not enhance the stiffness or reduce relative slip regardless of reinforcement ratio.

- Reducing the insulation thickness by 33% (from 150 to 100 mm [6 to 4 in.]) resulted in a 35% reduction in ultimate strength, while reducing it by 67% (from 150 to 50 mm [6 to 2 in.]) resulted in a 58% reduction. The end slip at the same load level was not affected much by the insulation thickness.

- The panel with X-pattern GFRP shear connectors with a 0.048% reinforcement ratio achieved a 32% degree of composite action, whereas the panels with transverse GFRP ties with a 0.0145% reinforcement ratio reached only 5% to 15% composite action. As a result, the panel with X-pattern connectors achieved 82% higher strength than the panels with transverse ties and, even more significantly, the deflection and relative slip for the panels with X-pattern connectors were less than 4% of the values for the panels with transverse ties.

- The primary failure mode of all panels was fracture of the transverse GFRP ties or diagonal shear connectors. A tension force developed in the transverse ties as the two wythes slipped relative to each other. The tension force along with a bend in the connectors at the concrete face caused failure. The diagonal connectors failed in both tension and compression. Despite the short 25 mm (1 in.) connector embedment, no pull-out failure was observed.

## Acknowledgments

The authors wish to acknowledge the financial support provided by the Canadian Precast/Prestressed Concrete Institute, KPM Industries for donating the UHPC, Tri-Krete and Spring Valley for fabricating the panels, and V-Rod for donating the GFRP reinforcing bars.

## References

1. PCI Committee on Precast Sandwich Wall Panels. 2011. "State of the Art of Precast/Prestressed Concrete Sandwich Wall Panels." *PCI Journal* 56 (2): 131–176.

2. Einea, A., D. C. Salmon, M. K. Tadros, and T. Culp. 1994. "A New Structurally and Thermally Efficient Precast Sandwich Panel System." *PCI Journal* 39 (4): 90–101.

3. Tomlinson, D., and A. Fam. 2014. "Experimental Investigation of Precast Concrete Insulated Sandwich Panels with Glass Fiber-Reinforced Polymer Shear Connectors." *ACI Structural Journal* 111 (3): 595–605.

4. Einea, A., D. C. Salmon, G. J. Fogarasi, T. D. Culp, and M. K. Tadros. 1991. "State-of-the-Art of Precast Concrete Sandwich Panels." *PCI Journal* 36 (6): 78–98.

5. Frankl, B. A., G. W. Lucier, T. K. Hassan, and S. H. Rizkalla. 2011. "Behavior of Precast, Prestressed Concrete Sandwich Wall Panels Reinforced with CFRP Shear Grid." *PCI Journal* 56 (2): 42–54.

6. McCall, W. C. 1985. "Thermal Properties of Sandwich Panels," *Concrete International* 7 (1): 35–41.

7. Tomlinson, D., and A. Fam. 2015. "Flexural Behavior of Precast Concrete Sandwich Wall Panels with Basalt FRP and Steel Reinforcement." *PCI Journal* 60 (6): 51–71.

8. Woltman, G., D. Tomlinson, and A. Fam. 2013. "Investigation of Various GFRP Shear Connectors for Insulated Precast Concrete Sandwich Wall Panels." *Journal of Composites for Construction* 17 (5): 711–721.

9. Pessiki, S., and A. Mlynarczyk. 2003. "Experimental Evaluation of the Composite Behavior of Precast Concrete Sandwich Wall Panels." *PCI Journal* 48 (2): 54–71.

10. Salmon, D. C., A. Einea, M. K. Tadros, and T. D. Culp. 1997. "Full Scale Testing of Precast Concrete Sandwich Panels." *ACI Structural Journal* 94 (4): 354–362.

11. Hassan, T. K., and S. H. Rizkalla. 2010. "Analysis and Design Guidelines of Precast, Prestressed Concrete, Composite Load-Bearing Sandwich Wall Panels Reinforced with CFRP Grid." *PCI Journal* 55 (2): 147–162.

12. Bush, T. D., and G. L. Stine. 1994. "Flexural Behavior of Composite Precast Concrete Sandwich Panels with Continuous Truss Connectors." *PCI Journal* 39 (2): 112–121.

13. Kim, J. H., and Y. C. You. 2015. "Composite Behavior of a Novel Insulated Concrete Sandwich Wall Panel Reinforced with GFRP Shear Grids: Effects of Insulation Types." *Materials* 8 (3): 899–913.

14. Tomlinson, D. G. 2015. "Behaviour of Partially Composite Precast Concrete Sandwich Panels under Flexural and Axial Loads." PhD thesis, Department of Civil Engineering, Queen's University, Kingston, ON, Canada.

15. Maximos, H. N., W. A. Pong, M. K. Tadros, and L. D. Martin. 2007. "Behavior and Design of Composite Precast Prestressed Concrete Sandwich Panels with NU-Tie." Final report, University of Nebraska–Lincoln.

16. Rizkalla, S. H., D. Lunn, G. Lucier, L. Sennour, H. Gleich, and J. Carson. 2013. "Innovative Use of FRP for Sustainable Precast Structures: Using Carbon-Fiber-Reinforced Grids in Walls and Other Components." *Precast Concrete Façade Tectonics Journal* 1 (8): 55–63.

17. Baby, F., B. A. Graybeal, P. Marchand, and F. Toutlemonde. 2012. "UHPFRC Tensile Behavior Characterization: Inverse Analysis of Four-Point Bending Test Results." *Materials and Structures* 46 (8): 1337–1354.

18. Graybeal, B. A. 2006. *Material Property Characterization of Ultra-High Performance Concrete.* Publication no. FHWA-HRT-06-103. McLean, VA: Federal Highway Administration.

19. AFGC (French Association of Civil Engineers). 2002. *Ultra High Performance Fibre-Reinforced Concretes, Interim Recommendations*. Paris, France: AFGC.

20. ASTM Subcommittee C09.61. 2011. *Standard Test Method for Splitting Tensile Strength of Cylindrical Concrete Specimens.* ASTM C496/C496M-17. West Conshohocken, PA: ASTM International.

21. Meng, D., T. Huang, Y. X. Zhang, and C. K. Lee. 2017. "Mechanical Behaviour of a Polyvinyl Alcohol Fibre Reinforced Engineered Cementitious Composite (PVA-ECC) Using Local Ingredients." *Construction and Building Materials* 141: 259–270.

22. CSA (Canadian Standards Association). 2012. *Design and Construction of Building Structures with Fibre-Reinforced Polymers*. CSA-S806. Toronto, ON, Canada: CSA.

23. Bentz, E. C. 2000. "Sectional Analysis of Reinforced Concrete Members." PhD thesis, Graduate Department of Civil Engineering, University of Toronto.

## Notation

$d$ = depth of the specimen

$d_0$ = reference depth of the specimen based on the experimental test

$f_{ct}$ = actual tensile cracking strength of concrete

$f_{ct,flexure}$ = measure tensile cracking strength of concrete

$K_u$ = degree of composite action in sandwich panels

$M_u$ = experimentally measured ultimate moment of the partially composite panel

$M_{u,FC}$ = theoretical ultimate moment for the fully composite case of the panel being considered

$M_{u,NC}$ = theoretical ultimate moment for the noncomposite case of the panel being considered

## About the authors


Valon Sylaj is a PhD candidate in the Department of Civil Engineering at Queens University in Kingston, ON, Canada.

Amir Fam is a professor, associate dean of research, and Donald and Sarah Munro Chair in Engineering and Applied Science at Queens University.

Malcolm Hachborn is chief engineer at M. E. Hachborn Engineering in Barrie, ON, Canada.

Robert Burak is president of the Canadian Precast/Prestressed Concrete Institute.


## Abstract


This paper presents a flexural experimental investigation of a new double-wythe panel design using ultra-high-performance concrete. Very thin (25 mm [1 in.]) wythes were used with a layer of extruded polystyrene core ranging from 50 to 150 mm (2 to 6 in.) in thickness, a design that is significantly lighter in weight than conventional panels. A total of eight 3000 × 600 mm (120 × 24 in.) panels, including one with steel fibers and seven with polyvinyl alcohol (PVA) fibers, were tested in four-point bending. Six of the eight panels with PVA fibers included additional mesh reinforcement in the wythes. The reinforcement was made of 4.2 mm (0.17 in.) diameter glass-fiber-reinforced polymer (GFRP) reinforcing bars with spacing that provided a longitudinal reinforcement ratio ranging from 0.28% to 0.92%. Two panel designs were considered in this study: a very low-composite design intended for minimal thermal bowing and a design with moderate composite action for enhanced flexural performance. The low-composite design used 4.2 mm GFRP transverse ties with only a 0.0145% reinforcement ratio, while the moderate-composite design used a heavier (0.048%) tie reinforcement ratio of the same reinforcing bars but oriented in diagonal configurations. The panel with PVA fibers achieved 48% of the flexural strength compared with the panel with steel fibers. Panels with mesh reinforcement achieved on average 78% higher strength than the panel with fibers only, regardless of reinforcement ratio. As insulation tripled in thickness, flexural strength increased 2.4 times. The calculated degree of composite action in panels with transverse ties was 5% to 15%, while that of the panel with diagonal ties was 32%.



## Keywords

Extruded polystyrene, GFRP, glass-fiber-reinforced polymer, insulation, ties, UHPC, ultra-high-performance concrete, wall, wythe, XPS.


## Review policy

This paper was reviewed in accordance with the Precast/Prestressed Concrete Institute's peer-review process.

## Reader comments

Please address any reader comments to *PCI Journal* editor-in-chief Tom Klemens at tklemens@pci.org or Precast/Prestressed Concrete Institute, c/o *PCI Journal*, 200 W. Adams St., Suite 2100, Chicago, IL 60606.